MNE 16 (2022) 100157

Contents lists available at ScienceDirect

Micro and Nano Engineering

journal homepage: www.sciencedirect.com/journal/micro-and-nano-engineering

Ionic diode desalination: Combining cationic Nafion™ and anionic Sustainion™ rectifiers

Zhongkai Li [a], Tianting Pang [b], Junjie Shen [b], Philip J. Fletcher [c], Klaus Mathwig [d], Frank Marken [a,*]

[a] Department of Chemistry, University of Bath, Claverton Down, Bath BA2 7AY, UK
[b] Department of Chemical Engineering, University of Bath, Claverton Down, Bath BA2 7AY, UK
[c] University of Bath, Materials & Chemical Characterisation Facility MC^2, Bath BA2 7AY, UK
[d] Stichting imec Nederland within OnePlanet Research Center, Bronland 10, 6708, WH, Wageningen, the Netherlands

ARTICLE INFO

Keywords:
Iontronics
Impedance
Ionic circuits
Conductivity
Seawater
Performance

ABSTRACT

Microscale ionic rectifier effects are commonly observed in devices based on semipermeable ionomer coated on an array of microholes with potential applications in alternating current (AC) driven desalination and/or electroosmotic pumping. The efficiency of devices is dependent on ionic diode switching speed, the rectification ratio, and the design of materials and the ionic circuit. Here, a new circuit is proposed based on coupling in parallel (i) a cationic diode based on the cation conductor Nafion and (ii) an anionic diode based on the anion conducting Sustainion. With an alternating driving voltage, a net desalination effect is observed without any moving parts and without significant side reactions. Experimentally, a 4-electrode configuration and a 2-electrode configuration are compared. The ionic diode desalination system is shown to work with only two carbon mat driver electrodes, but the performance in particular at higher ionic strengths (>10 mM) still needs to be improved. Based on the experimental prototype, the current/power efficiency are investigated and challenges for future improvements are discussed.

1. Introduction

Innovation in desalination processes is important [1] on a big industrial plant scale but also on smaller scale for smaller communities, individual households, or for emergency water provision. A range of technologies exist energised by pressure or by applied electrical power [2] or by exploiting thermal gradients [3], but new innovative approaches still emerge (*e.g.* based on novel nanoporous bio-materials [4]) to help meeting the challenge of water purification/provision for the future. Electrical power applied to membranes can be delivered as a constant applied voltage (leading to unwanted reactions at driver electrodes) or as an alternating voltage (employing capacitive charging of driver electrodes to avoid redox reactions). When using alternating voltage, the membrane needs to act as rectifier. This can be achieved with ionic circuits.

Ionic circuitry [5], [6] and ionic components in fluidic devices can be considered bio-mimetic [7] or bio-inspired [8] and are of considerable importance in energy conversion mechanisms [9] [10] [11], in sensing [12], and in selective ion transport [13] and desalination [14]. The principal element in ionic circuits is the ionic diode [15], which is employed here for a desalination process. In contrast to conditions in classic direct current (DC) electrodialysis, the rectifying functionality of the ionic diode introduces an element of irreversibility, which is the key to transforming electrical energy input (as alternating current AC) into ion gradient energy or into a salt gradient (similar to electronic diodes operating in a rectifier to transform AC electrical input into DC electrical output). Importantly, AC driven processes with ionic diodes can be designed to operate without any moving parts and to minimise energy losses, for example, due to unwanted electrolytic reactions. In a recent review, ionic diode desalination has been indicated as a potentially new and interesting water purification technology [[16]. The concept of "iontronics" [17], [18] has been suggested as a way to develop complexity in ionic circuitry similar to that now common in electronics. Here, we present evidence for coupling an anionic diode and a cationic diode in a circuit to create desalination functionality.

In our recent work, we reported the ease of producing microscale ionic rectifiers based on semipermeable materials (such as Nafion [19], bacteriophage [20], graphene oxide [21], nanocarbon mats [22],

* Corresponding author.
E-mail address: f.marken@bath.ac.uk (F. Marken).

https://doi.org/10.1016/j.mne.2022.100157
Received 8 February 2022; Received in revised form 31 May 2022; Accepted 25 June 2022
Available online 30 June 2022

cellulosic materials [23], or polymers of intrinsic microporosity [24]) deposited on microhole substrates [25]. Realising that a combination of ionic rectifiers and ionic resistors can be employed in desalination [26], we reported a first prototype based on a 4-chamber ionic circuit design [27]. This design was hampered by the need for an efficient ionic resistor (a commercial anion conducting membrane was employed but also shown to rapidly degrade). Every resistor introduces energy losses and therefore substantial improvements in the ionic circuit design are still possible by removing resistors. Here, a 2-chamber system is proposed based only on a combination of a suitable complementary pair of a cationic diode and an anionic diode without ionic resistors. We demonstrate/compare a cationic diode based on Nafion (a commercial cation conductor) and an anionic diode based on Sustainion (a commercial anion conductor). When combining Nafion and Sustainion into a single membrane, desalination and salination processes occur simultaneously in a 2-chamber device when driven by an AC voltage.

Both Nafion and Sustainion are commercially available materials supplied as readily processable solutions dispersed in alcohol/water. Nafion (see molecular structure in Fig. 1A) has been employed widely and is a well-characterised cation conducting ionomer [28]. Sustainion (see molecular structure in Fig. 1B) has been developed more recently [29] in particular for applications in carbon dioxide electroreduction [30]. As an imidazolium-based ionomer, Sustainion exhibits excellent anion semi-permeability. It is shown here that similar to Nafion providing cationic diodes, Sustainion provides anionic diodes with good rectification properties and durability. A combination of cationic Nafion diode and anionic Sustainion diode is shown to allow desalination/salination processes to be driven with carbon mat electrodes.

Fig. 2 illustrates the operation of a 2-chamber system (two electrolyte-filled compartments connected *via* ionic diodes) with a membrane separating left and right compartment. With a positive bias voltage applied on the right hand side (in this report right corresponds to the working electrode) the cationic diode opens to allow cation transport from right to left. With a negative bias voltage applied on the right the anionic diode opens to allow anion transport from the right to the left. Over a complete polarisation cycle, the net effect is the transport of salt (both anions and cations) from the right compartment (desalination) into the left compartment (salination).

The suggested 2-chamber desalination system only requires two driver electrodes (for example carbon mats) and no moving parts. Theoretically (for sufficiently high frequencies), there should be insignificant side reactions due to electrolysis at the driver electrodes and therefore no energy should be lost in electrolysis and formation of side products. This report provides proof-of-concept data for a simple 2-chamber ionic circuit for desalination/salination driven with AC electricity.

2. Experimental

2.1. Chemical reagents

Nafion perfluorinated ion-exchange resin (5 wt%) was purchased from Sigma-Aldrich. Sustainion dispersion XC-2 (5 wt%) was purchased from The Fuel Cell Store (www.fuelcellstore.com). Agarose powder was purchased from Melford Ltd. And sodium chloride (99.5%) and sodium hydroxide (pellets) were purchased from Fisher Scientific Ltd. All chemicals were utilised without further purification. Ultra-pure water was used for preparation of all aqueous solutions, from a Thermo Scientific water purification system with a resistivity not <18.2 MΩ cm (20 °C).

2.2. Instrumentation

Electrochemical measurements were conducted with an Autolab PGSTAT30 (Metrohm Ltd.) for cyclic voltammetry and chronoamperometry or a Solartron Analytical ModuLab XM MTS system for impedance spectrometry, either in 4-electrode or in 2-electrode configuration. The cell contained two cylindrical half-cells which were separated by a membrane-coated, laser-drilled Teflon substrate (5 μm thick, Laser Machining Ltd., Birmingham, UK). Reference and sense electrodes were silver wires (0.5 mm thickness, Advent Ltd. research materials) and working and counter electrode were based on activated carbon fibre electrodes (1 cm^2, FLEXZORB FM50K, from Chemviron Carbon Cloth Division, UK) with 130 g m^{-2} surface density, 0.5 mm thickness, and Brunauer-Emmett-Teller nitrogen adsorption surface area of 1220 m^2g^{-1}. The working and sense electrodes were placed on the membrane side of the cell (right hand side) in all experiments. Measurements of solution conductivity were carried out on a S30 SevenEasy Conductivity

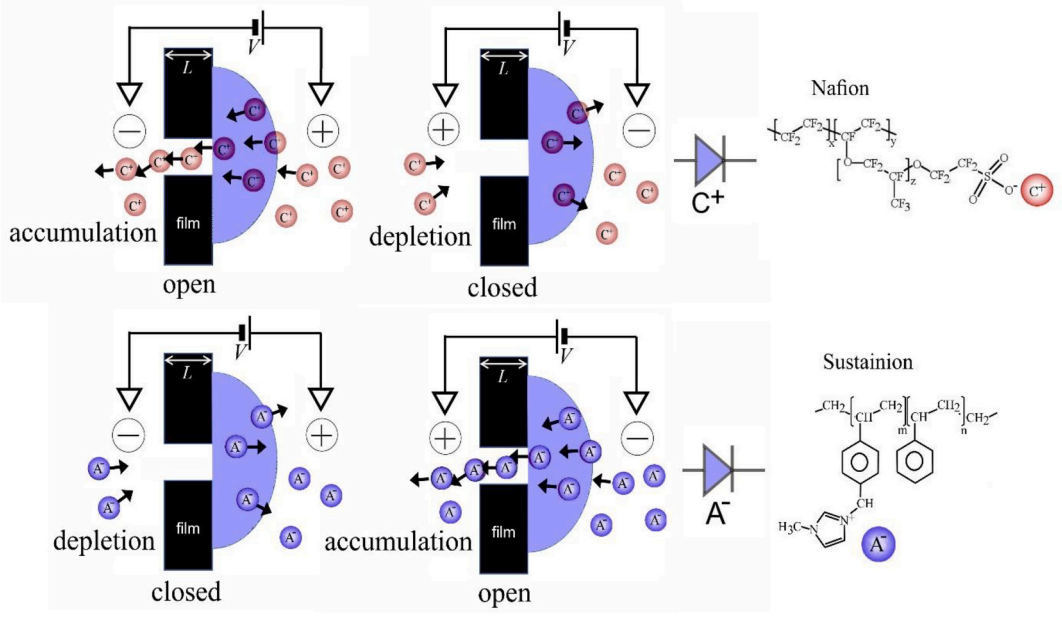

Fig. 1. Schematic illustration of the Nafion cationic diode switching between open (accumulation) and closed (depletion) states. Similarly, an illustration is shown for the sustainion anionic diode switching between open and closed states. The molecular structures for Nafion and Sustainion XC-2 are indicated.

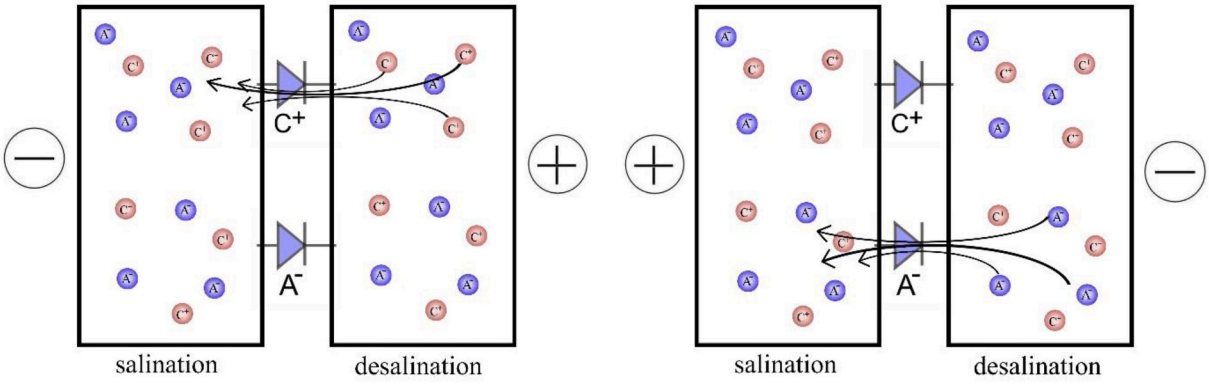

Fig. 2. Illustration of the effect of positive or negative bias voltages applied to a 2-chamber system with a membrane composed of a combination of cationic and anionic diode.

Meter. Scanning electron microscope images were taken using a Hitachi SU390 with attached Oxford Instruments Ultim Max 170mm^2 EDX detector.

2.3. Procedures

2.3.1. Membrane preparation

The membrane film was prepared by deposition of ionomer materials onto either (i) a single microhole or (ii) an array of 10 × 10 microholes (see Fig. 3; 5 μm thick Teflon, Laser Machining Ltd., Birmingham, UK). For Sustainion, a drop of 10 μL of Sustainion solution (5 wt%) was placed onto the microhole array (on an agarose gel substrate [19] to prevent the ionomer solution from penetrating through microholes). After drying, the ionomer deposit was covered with a drop of 1 M NaOH solution for 10 min to condition the Sustainion film (by ion exchange to open the ion-channels). Based on previous fluorescence microscopy studies [19] the thickness of the resulting Nafion or Sustainion films is estimated to be 5 ± 2 μm. After rinsing the alkaline solution, the cell was assembled (see Fig. 3). For Nafion, a drop of 10 μL of Nafion solution (5 wt%) was placed onto the microhole (on agarose gel). Once evaporated to dryness, the Teflon film was removed from the agarose substrate and assembled into the electrochemical cell.

2.3.2. Electrochemical cell assembly

The electrochemical characterisation (for single microhole membranes) of cationic Nafion diodes and anionic Sustainion diodes was performed in a "U-cell" (see Fig. 3A). Typically, 10, 100, or 500 mM aqueous NaCl solution were applied symmetrically in the two half-cells for measurements with cyclic voltammetry, chronoamperometry, or impedance spectrometry. For desalination experiments (employing two arrays of 10 × 10 microholes), the Teflon membrane was coated with both Nafion and Sustainion (see Fig. 3C and Fig. 4). The Sustainion deposit was pre-treated with 0.1 M NaOH solution before the cell was assembled. The presence of Nafion and Sustainion is documented in Fig. 4 based on scanning electron microscopy (SEM) and energy dispersive x-ray (EDX) elemental mapping. Sustainion shows a clear

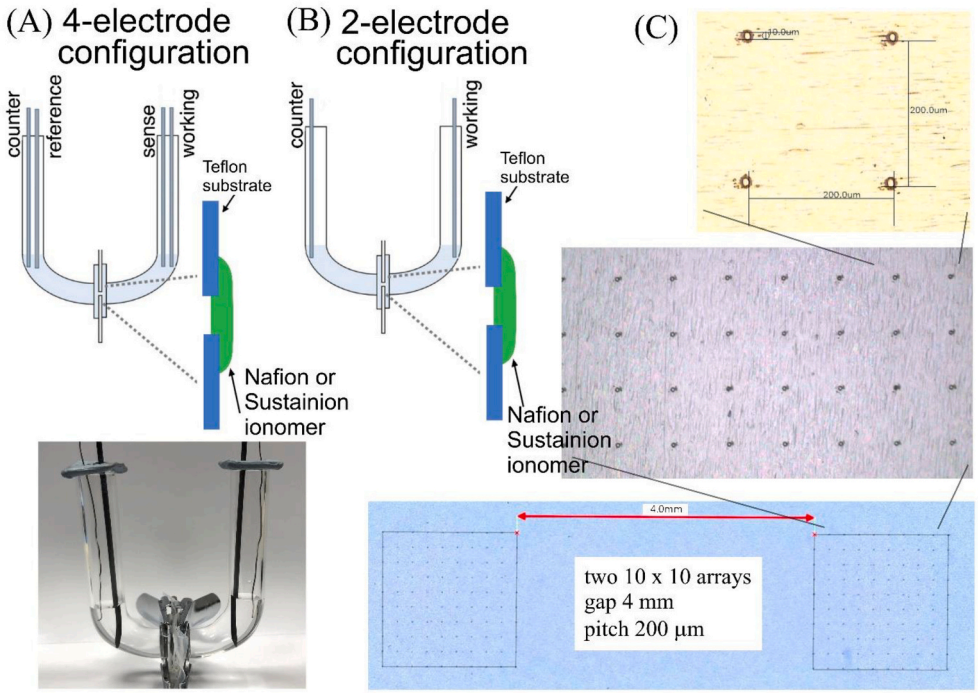

Fig. 3. (A) Schematic of the 4-electrode configuration with working and sense electrodes in the right compartment and counter and reference electrode in the left compartment (Photograph shown below). (B) Schematic of the 2-electrode configuration with only working and counter electrode. (C) Optical micrographs showing two 10 × 10 arrays in a 5 μm thick Teflon film.

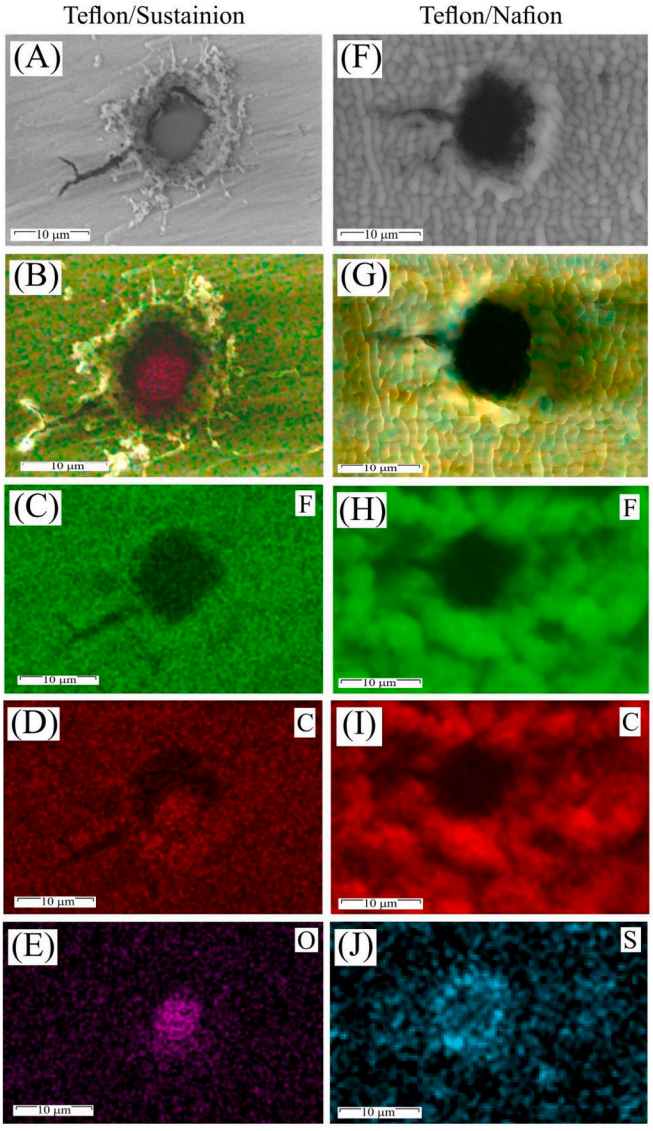

Fig. 4. (A) Scanning electron microscopy (SEM, backscatter) image of the backside of a Sustainion coated Teflon film with 10 μm diameter microhole. (B-E) EDS mapping for F, C, O. (F) SEM image of the backside of a Nafion coated Teflon film with microhole. (G-J) EDS mapping for F, C, S. Images (B) and (G) are layered X-ray images combining images C—D and H-J.

oxygen signature, whereas Nafion shows a sulfur signature (compare molecular structures in Fig. 1).

Reinforcement rings (outer diameter 13 mm, inner diameter 6 mm, sticky plastic used for folders, www.3Loffice.com) were employed to mechanically stabilise the Teflon film membrane. Aqueous NaCl solution (volume 5 mL) was added on both sides of the cell. The cell voltage was then applied with constant potential pulses (square wave, typically with 10 s duration) to enable the one-way movement of ions. For 10 mM NaCl solution, ±2 V was applied for a 4-electrode configuration, and ± 5 V for both 4-electrode and 2-electrode configurations (150 min total desalination time). For 100 mM NaCl solution, ±2 V was applied for a 4-electrode configuration (270 min desalination time). For 500 mM NaCl solution, ±2 V was applied. The change of salt concentration was monitored by regularly measuring the conductivity of electrolyte solutions in both compartments.

2.3.3. Conductivity measurements

During desalination experiments the salt content in the left and right compartments were followed by measuring ionic conductivity (S30 SevenEasy Conductivity Meter). In regular intervals the desalination process was stopped, samples of 1 mL were taken, measured, and returned, for the desalination experiment to continue.

3. Results and discussion

3.1. Cationic Nafion diodes versus anionic Sustainion diodes I.: electrochemical characterisation

Both ionomer materials, Nafion and Sustainion, were applied from solution with approx. 5 μm thickness onto the 5 μm thick Teflon substrate with a single 10 μm diameter hole. Nafion as a well-known cation conducting material is anticipated to generate a cationic diode [19], whereas Sustainion as an anion conducting material is expected to result in anionic diode behaviour (after initial activation of the anion conducting channels). Fig. 5A shows cyclic voltammograms for Sustainion immersed in aqueous NaCl. The ionic diode switches from "open" for negative applied potentials to "closed" for positive applied potentials consistent with anionic diode behaviour (see Fig. 1B). Voltammetric data are close to steady state (due to steady state diffusion towards the 10 μm diameter microhole) and dependent on the electrolyte concentration. An increase in the NaCl concentration causes both an increase in ionic current and a weakening of the ionic diode effect. The rectification ratio estimated at ±2 V is typically 14–15 for 0.01 M, 10–15 for 0.1 M, and 3–5 for 0.5 M NaCl. Higher ionic strength (i) compromises semipermeability, and (ii) changes the mode of resistivity [31], and therefore overall weakens the rectification effect.

Fig. 5B shows cyclic voltammograms for Nafion deposited onto a 10 μm diameter microhole in Teflon. The ionic diode effect is observed and the open state at positive applied potentials is consistent with a cationic diode (Fig. 1). For Nafion the rectification current ratios at ±2 V are 65–70 for 0.01 M, 22–24 for 0.1 M, and 6–7 for 0.5 M NaCl. Although the rectification effect weakens for higher concentrations of electrolyte, there is still a significant effect even at a concentration of 0.5 M NaCl. The loss of rectification at higher ionic strength could be associated with some loss of semipermeability (an increase in transport of anions in addition to predominant transport of cations) and a decrease in the extent of the Debye layer [32]. This is not a major factor in fuel cell Nafion membrane performance [33] but does affect rectification particularly for membranes with bigger pores [34].

Fig. 5C and D demonstrate that the steady state behaviour of the diodes is maintained for a scan rate of 0.5 Vs^{-1} (consistent with quasi-steady state diffusion processes at the 10 μm diameter microhole; for comparison, the approach to steady state (within 5%) for a 10 μm diameter inlaid disk microelectrode can be estimated as about 1 s [35]). The voltage range can be extended to ±5 V without deterioration of the ionic diode behaviour for both Nafion and Sustainion (*vide infra*).

Chronoamperometry data (see Fig. 6) demonstrate the approach to steady state as a function of time and of NaCl concentration. For Sustainion the steady state is reached in typically 1 s with current spikes indicating the switching process in which NaCl diffuses into (accumulation) or out of (depletion) the microhole region (see Fig. 1A). Data for Nafion (Fig. 6D-F) exhibit more complexity with a change in transient shape during accumulation at low concentration (a rising transient) and at high concentration (a falling transient).

In order to gain deeper insight into the ionic diode behaviour in different time domains, electrochemical impedance spectra were recorded (Fig. 7) with a bias voltage of 0.0 V and over a frequency range of 1 Hz to 100 kHz.

For the anionic Sustainion diode in 0.01 M NaCl, two semi-circular features are identifiable in the Nyquist plot (Fig. 7A). The high frequency semicircle has been attributed to the capacitive charging of the Teflon substrate *via* ion transport through the microhole. The associated capacitor is typically 0.4 nF in all data sets (typical for charging of the 5 μm thick Teflon film). R_s is essentially zero (within error) due to the 4-

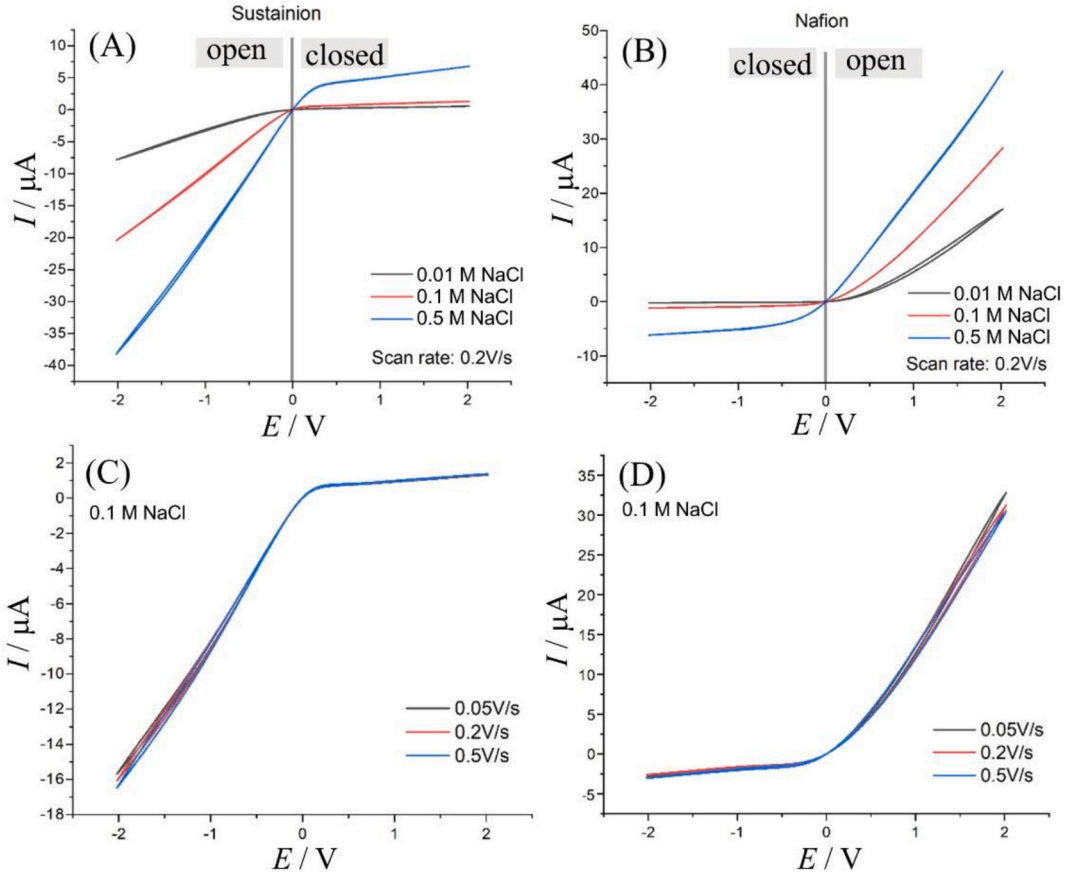

Fig. 5. (A) Cyclic voltammograms (scan rate 0.2 Vs^{-1}) for Sustainion in 0.01, 0.1, and 0.5 M NaCl. (B) As before for Nafion. (C) Cyclic voltammograms (scan rates 0.05, 0.2, and 0.5 Vs^{-1}) for Sustainion in 0.1 M NaCl. (D) As before, for Nafion.

electrode cell configuration. The value for R_p reflects predominantly ionomer resistivity at high frequency, which decreases with increasing NaCl concentration. The value is likely to be dominated by the Sustainion film resistivity but also includes aqueous electrolyte conductivity in the microhole region. Accordingly, the time constant for the first semicircle $\tau = C \times R_p = 1/\omega_{max}$ decreases from about 1 ms to 0.1 ms with higher electrolyte concentration. Perhaps more interesting/relevant is the second semi-circular feature, which is associated with the switching of the diode from open to closed state and *vice versa*. For Sustainion a value of $\omega_{max} = 10$ Hz is typical and independent of the electrolyte concentration. This frequency describes the switching time of the diode between open and closed states. The value is consistent with chronoamperometry data in Fig. 6 (the switching time $\tau = 1/\omega_{max}$ corresponds to approx. 34% approach to steady state).

For Nafion coated on a single microhole (Fig. 7D-F), a similar pattern emerges. Two semi-circular features are detected with the higher frequency data being associated with the charging of the Teflon film. The variation in ω_{max} is linked to electrolyte and ionomer resistivity. The lower frequency feature occurs with typically $\omega_{max} = 10$ Hz independent of electrolyte concentration and is therefore attributed to the open-closed switching of the ionic diode (by diffusion-migration of electrolyte into the microhole region). Both Nafion and Sustainion diodes exhibit very similar behaviour and are therefore suitable to be combined into an ionic circuit for desalination. However, for this desalination process to be effective, a single microhole device would not work. An array of ionic diodes is required. In the design of the array, it is assumed that separating individual microholes by 20 × the microhole diameter will create close to diffusionally independent diodes for each of the microholes.

3.2. Cationic Nafion diodes versus anionic Sustainion diodes II.: ionic diode desalination

When going from a single microhole to an array of 100 microholes (see Experimental), the net current is increased accordingly, but the rectification effect remains as long as the individual ionic diodes are spaced sufficiently far of each other and as long as additional resistivity modes do not suppress currents. Here, two separate arrays are coated from the same side with Nafion (10 × 10 microholes, 200 μm pitch) and with Sustainion (10 × 10 microholes, 200 μm pitch). Fig. 8A shows data for cyclic voltammetry immersed in 0.01 M NaCl. Substantial currents are observed (typically a factor 20 higher compared to those for single microhole diodes) in the negative potential range (the anionic diode is open: anion transport dominates) and in the positive potential range (the cationic diode is open: cation transport dominates). The slightly lower than expected open currents are attributed resistivity modes due to cell design (the tube cylindrical diameter introducing resistivity). Fig. 8B shows chronoamerometry data switching between -2 V (anion transport) and + 2 V (cation transport). The limiting currents are consistent with those in cyclic voltammetry data and when operating for a prolonged period of time (150 min) only insignificant changes in performance are observed.

Fig. 8C shows chronoamperometry data obtained with an applied voltage of -5 V (anion transport) and + 5 V (cation transport) and in this case some deterioration of the signal is observed. The negative current (anion transport) appears to increase with time, which may be linked to gradual structural changes in either the Nafion or the Sustainion film in the device. This result suggests that operation at a higher applied voltage can affect the performance of the diodes.

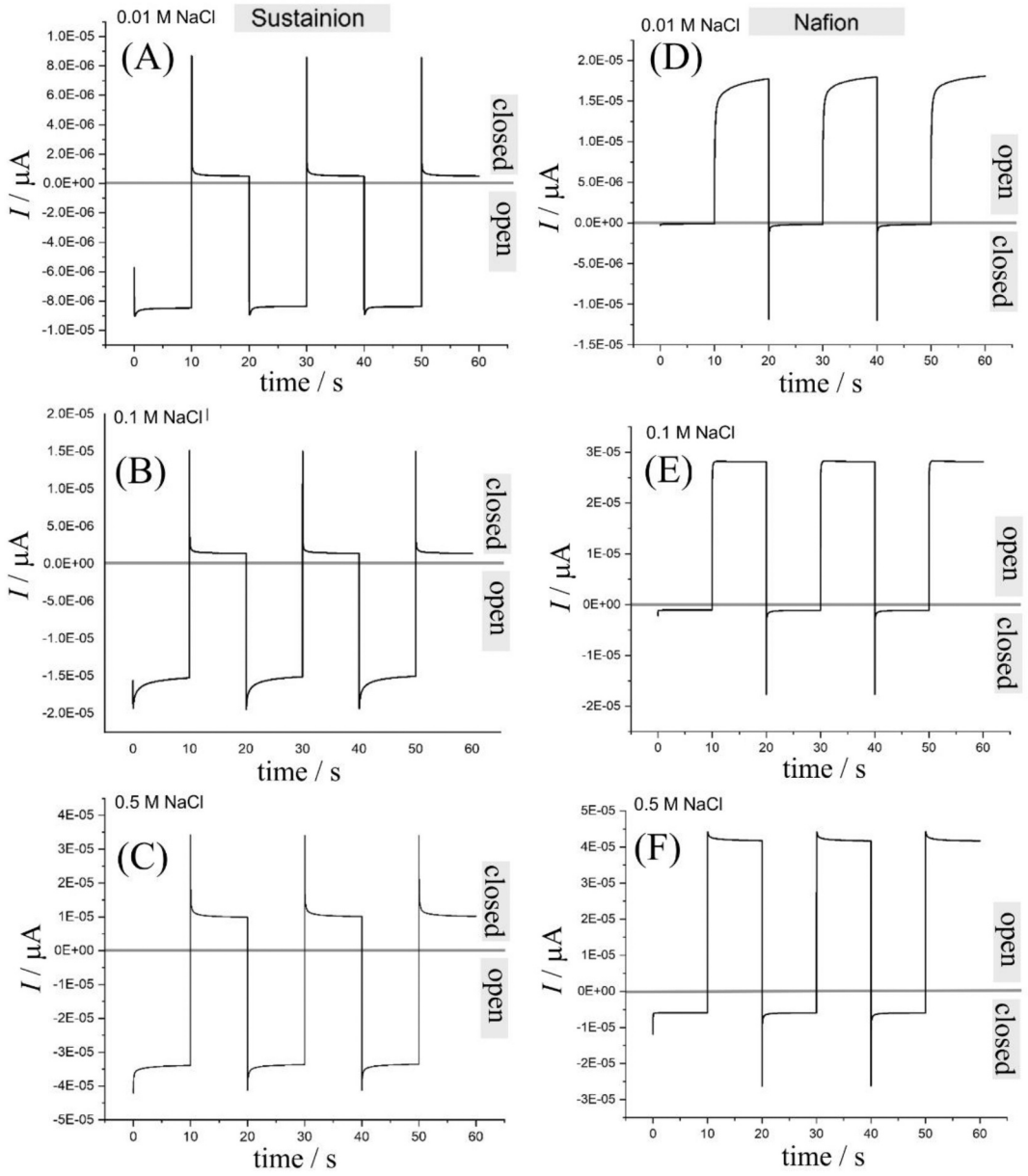

Fig. 6. Chronoamperometry transients (single microhole devices with 10 µm diameter) for (A-C) Sustainion and (D—F) Nafion in 0.01 M NaCl (A,D), 0.1 M NaCl (B, E), and 0.5 M NaCl (D,F).

3.3. Cationic Nafion diodes versus anionic Sustainion diodes III.: 4-electrode versus 2-electrode configuration

Fig. 8D shows data obtained under the same conditions but with a 2-electrode configuration (see Experimental). For practical applications of the ionic diode desalination process, reference electrodes are not essential and rather costly. When applying a voltage directly to the carbon mat electrodes and without reference electrodes, some fraction of the applied voltage is lost at the carbon electrolyte interface (here, the exact applied voltage to the membrane is not known). This can be verified based on the somewhat lower current (30% lower) for both anion and cation pumping. Although the data suggest that a 2-electrode configuration can be employed for the desalination process, there is a loss of energy associated with the driver electrode process. The 2-electrode configuration (in contrast to the 4-electrode configuration) allows the true energy consumption (voltage × current) in the process to be verified.

The degree of desalination was followed as a function of time by measuring the ionic conductivity of the electrolyte solution in the left and in the right compartment (see Experimental). With 0.01 M NaCl the initial specific conductivity at room temperature was 986 µS cm^{-1} (= 100%; this value is consistent with previous reports [27]). Fig. 9A shows the relative change in conductivity with desalination time (switching from +2 V to -2 V in 10 s intervals; average current 0.2 mA). Clearly, in the left compartment (see Fig. 9A) salt is accumulated and in the right compartment salt is depleted (in agreement with the mechanism indicated in Fig. 2). Given the size of the microhole array, the desalination process is slow and requires hours. However, when comparing the desalination rate observed experimentally and that anticipated based on 100% current efficiency (see red line in Fig. 9A), the process is approximately 80% current efficient. That is, 20% of current is lost due to switching of the diode and some ion back-flow. This value seems encouraging as a starting point for further optimisation.

When increasing the salt concentration to 0.1 NaCl and employing ±2 V in 4-electrode configuration, a similar trend is observed (initial conductivity 9040 µS cm^{-1} = 100%; average current 1.1 mA). The

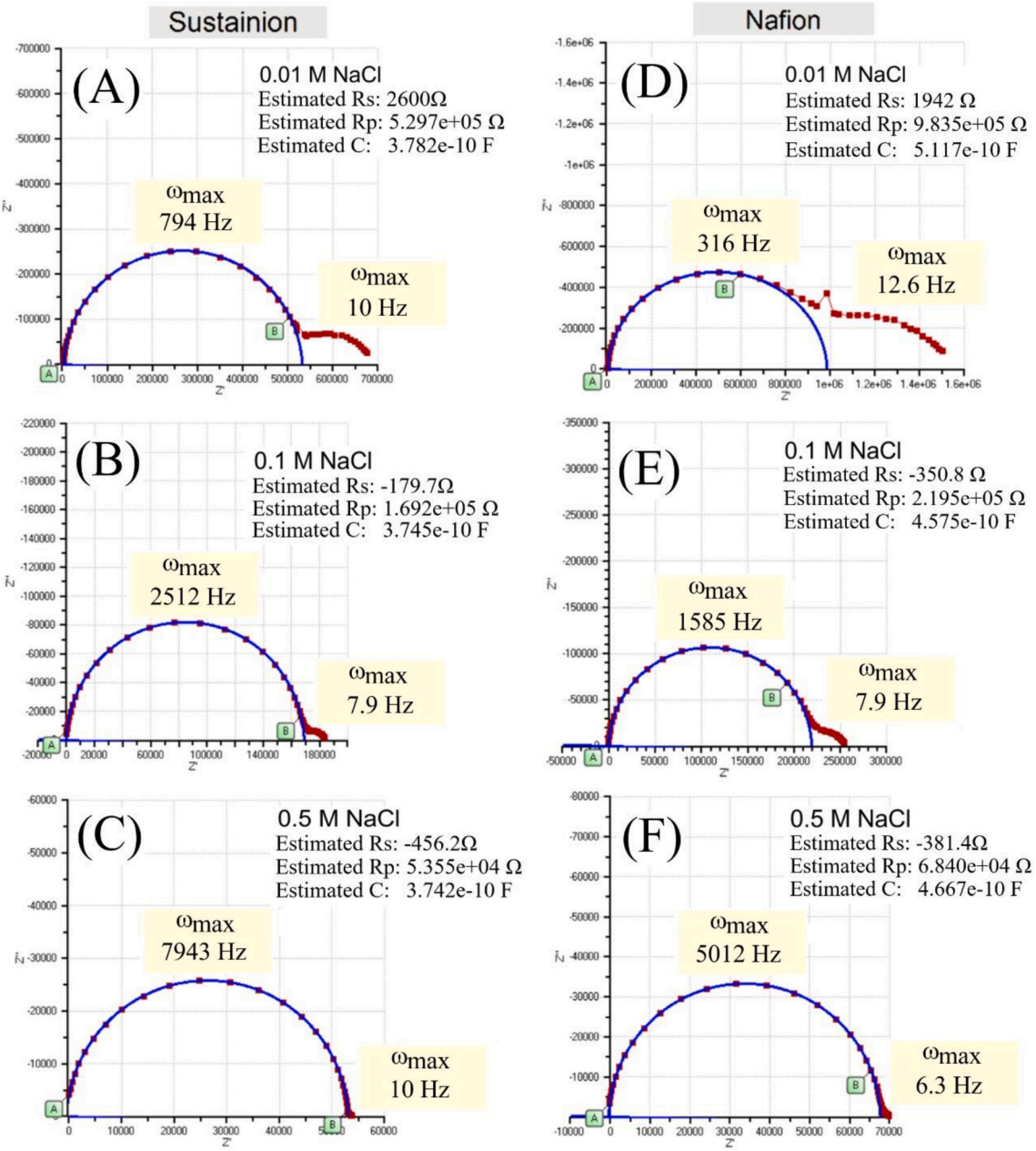

Fig. 7. Electrochemical impedance data (4-electrode configuration; frequency range 1 Hz to 100 kHz; bias 0.0 V; 25 mV amplitude, single microhole 10 μm diameter) in aqueous 0.01 M, 0.1 M, and 0.5 M NaCl for (A-C) Sustainion and (D—F) Nafion deposits on 10 μm diameter microhole in 5 μm thickness Teflon. Data fitting parameters based on $R_s(R_pC)$ elements.

desalination current in this case is increased, but the presence of the higher salt concentration counter-balances this effect to give an apparently slower rate of desalination (Fig. 9A). A slight imbalance in the desalination/salination effect is likely to be associated with electrolytic processes at the carbon mat electrodes when higher currents are applied (especially at higher ionic strength). The approximate current efficiency is significantly lower at about 40%. That is, now 60% of the current is lost due to diode switching and back-flow of ions.

Fig. 9B demonstrates the effect of the applied potential. As expected, the increase in potential leads to higher currents and therefore to a faster rate of desalination. For 10 mM NaCl solution and ± 5 V the average current is 0.53 mA. Over an hour, this corresponds to 1.9C, or a 2 mM change in concentration. This suggests approximately 50% current efficiency. Both, a higher electrolyte concentration and a higher applied voltage lower the current efficiency.

For practical applications of the ionic diode desalination approach, the 4-electrode configuration is less desirable compared to the 2-electrode configuration. Due to the loss of some voltage across the carbon mat | electrolyte interface, the performance in the 2-electrode configuration is lowered, but the process is still possible. Fig. 9C shows data for 0.01 M NaCl and ± 5 V driving voltage contrasting 4-electrode and 2-electrode configuration. The rate of desalination is approximately halved when using the 2-electrode configuration, but it is still higher compared to an experiment using ±2 V in 4-electrode configuration. This suggests that approximately half of the driving voltage is lost at the carbon mat | electrolyte interface. As a result, an imbalance in electrolyte composition can occur (see Fig. 9D) which is less severe for shorter pulses. In the future, losses due to voltage build-up at the carbon mat | electrolyte interface have to be considered and minimised for further optimisation.

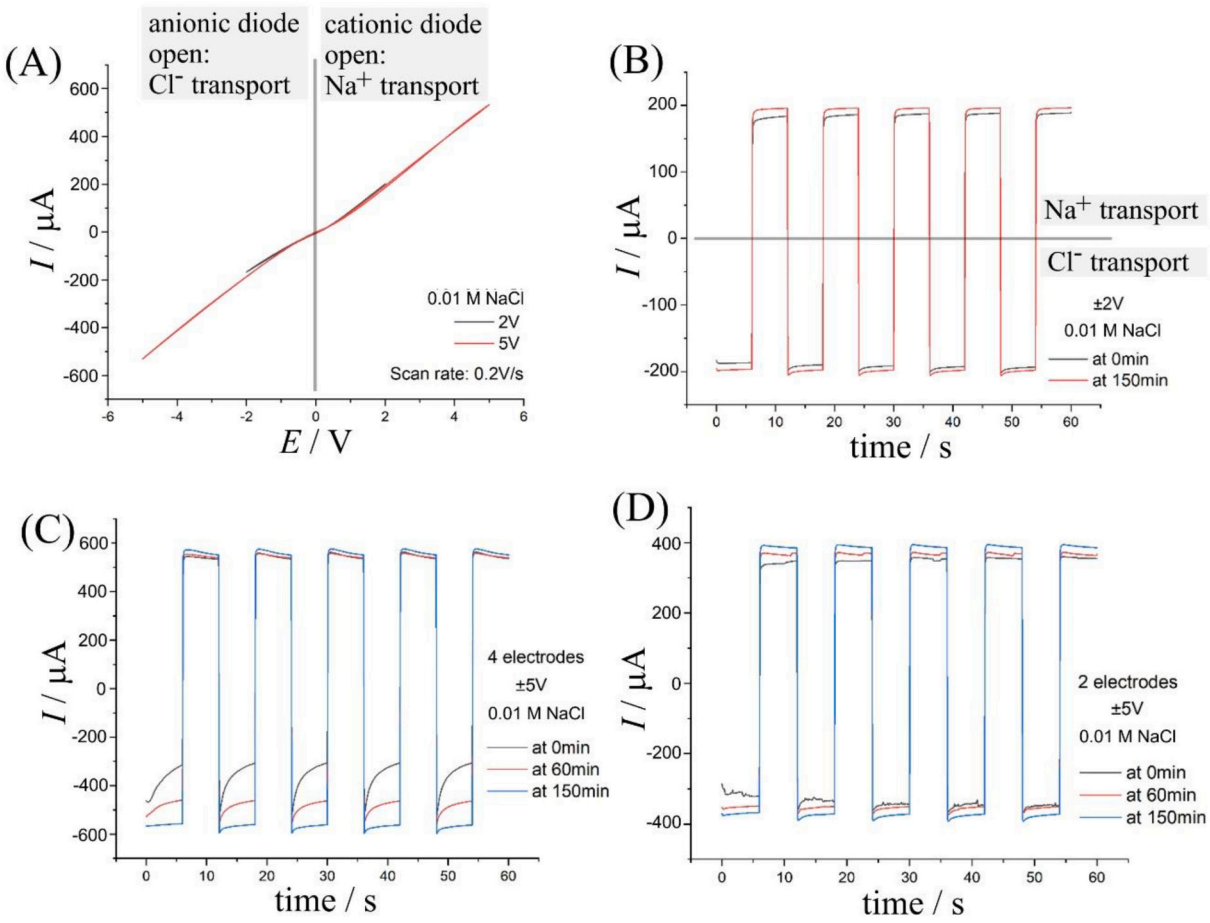

Fig. 8. (A) Cyclic voltammograms (scan rate 0.2 Vs^{-1}) for a double array (Nafion coated onto 10 × 10 microholes; Sustainion coated onto 10 × 10 microholes) immersed in 0.01 M NaCl. Potential regions dominated by anionic/cationic diode behaviour indicated. (B) Chronoamperometry employing ±2 V in 0.01 M NaCl before and after 150 min operation. Anionic/cationic diode behaviour indicated. (C) Chronoamperometry (4-electrode configuration) employing ±5 V in 0.01 M NaCl after (i) 0 min, (ii) 60 min, (iii) 150 min operation. (D) As before, but employing a 2-electrode configuration.

The energy efficiency of the ionic diode desalination approach will depend on various experimental parameters. For the 10 mM NaCl solution in Fig. 9A allows extrapolation to approximately 30 h operation for 90% desalination. This would require 22C electricity or 13 KJ energy per litre (assuming about 3 V applied; consistent with 3.6 $KWhm^{-3}$). This would incur electricity costs of 0.0004 $ per litre or 0.4 $ per cubic meter (assuming 0.12 $ per KWh) compared to about 1$ per cubic meter [36] for highly effective water desalination plants. For reverse osmosis energy consumption is approx. 4 $KWhm^{-3}$ [29]. Clearly, this comparison is premature and indeed unrealistic (comparing 90% salt removal compared to full desalination to high quality drinking water) but maybe useful as a starting point. The methodology will require a lot more work to allow a more meaningful assessment of operational costs and promise for specific applications.

4. Conclusion

It has been shown that for ionomer-covered microholes (i) Nafion allows cationic diode phenomena to be observed and (ii) Sustainion allows anionic diode phenomena to be observed. These complementary ionic diodes based on Nafion and Sustainion are formed on Teflon microhole substrates (10 µm diameter; either single microholes or 10 × 10 arrays). Both types of ionic diodes perform well in 0.01 M NaCl and still work even in 0.5 M NaCl. They can be combined into a 2-chamber desalination system, and this has been demonstrated in 4-electrode and in 2-electrode configuration (currently effective only for 0.01 M NaCl). This is a new example for an ionic circuit with elements (anionic diode and cationic diode) selected to create an overall function in desalination/salination. This approach, ionic diode desalination (IDD), is fundamentally different from other common approaches in desalination and the optimization/analysis of ionic circuits will provide and new tool in developing technologies.

The current efficiency of the ionic diode desalination process is dependent on the salt concentration as well as on the applied voltage. When operated at 10 mM NaCl, desalination effects are clearly demonstrated, and efficiency seems reasonable. When operated at higher salt concentrations, the efficiency drops considerably so that for 0.5 M NaCl this process is currently not possible. Problems have been identified in (i) some loss of rectification ratio and semipermeability when increasing the salt concentration; (ii) rectification in the ionic diode relies on high conductivity in the ionomer relative to the electrolytes solution and this also is compromised at higher ionic strengths; and (iii) more importantly electrolytic processes at the driver electrodes affecting the overall process. Higher surface area driver electrode based on porous carbon (super-capacitive or intentionally coated with a redox system) will be desirable and the pulse time needs to be lowered. Therefore, the switching time of ionic diodes also needs to be improved. There is no reason for the open/closed switching time not to be substantially improved with small diameter ionic diodes or with entirely new types of ionic diode mechanisms without the need for microholes [15]. In the future, much better combinations of materials and operational conditions will help improving performance.

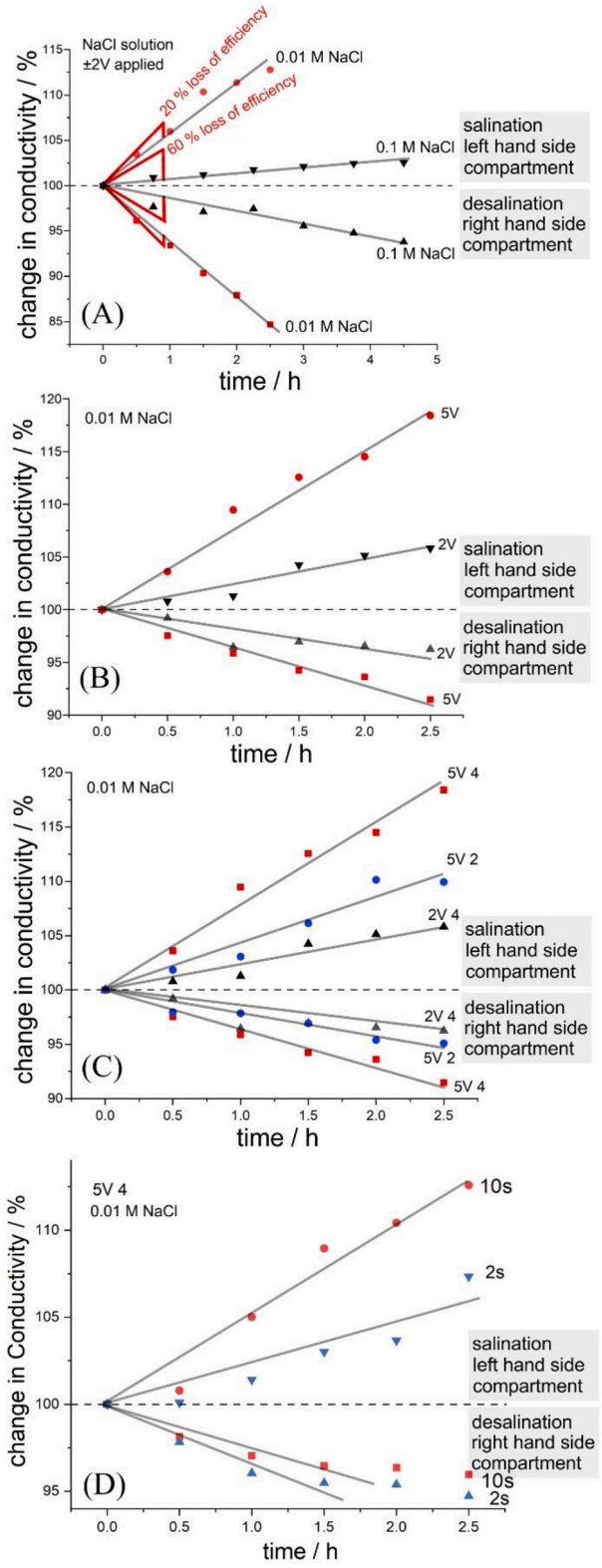

Fig. 9. Data for ionic conductivity in the left and right compartment of the ionic diode desalination system (Nafion and Sustainion coated onto 10 × 10 microhole arrays; applied potential pulses either ±2 V or ± 5 V with 10 s duration). (A) Comparison of data for 0.01 M and 0.1 M NaCl. (B) Comparison of ±2 V and ± 5 V driving voltage in 4-electrode configuration. (C) Comparison of data for 4-electrode and 2-electrode configuration. (D) Comparison of data for 4-electrode configuration, ±5 V, 10 s and 2 s pulse duration.

Declaration of Competing Interest

The authors declare that they have no known competing financial interests or personal relationships that could have appeared to influence the work reported in this paper.

Acknowledgements

F.M. thanks for the initial financial support by the EPSRC (EP/K004956/1).

References

[1] H. Nassrullah, S.F. Anis, R. Hashaikeh, N. Hilal, Energy for desalination: a state-of-the-art review, Desalination 491 (2020), 114569, https://doi.org/10.1016/j.desal.2020.114569.

[2] A. Subramani, J.G. Jacangelo, Emerging desalination technologies for water treatment: a critical review, Water Res. 75 (2015) 164–187, https://doi.org/10.1016/j.watres.2015.02.032.

[3] G. Gopi, G. Arthanareeswaran, A.F. Ismail, Perspective of renewable desalination by using membrane distillation, Chem. Eng. Res. Des. 144 (2019) 520–537, https://doi.org/10.1016/j.cherd.2019.02.036.

[4] Y.H. Teow, A.W. Mohammad, New generation nanomaterials for water desalination: a review, Desalination 451 (2019) 2–17, https://doi.org/10.1016/j.desal.2017.11.041.

[5] J. Li, D.Q. Li, Integrated iontronic circuits based on single nanochannels, ACS Appl. Mater. Interfaces 13 (40) (2021) 48208–48218, https://doi.org/10.1021/acsami.1c12324.

[6] R.A. Lucas, C.Y. Lin, L.A. Baker, Z.S. Siwy, Ionic amplifying circuits inspired by electronics and biology, Nat. Commun. 11 (1) (2020) 1568, https://doi.org/10.1038/s41467-020-15398-3.

[7] X. Hou, W. Guo, L. Jiang, Biomimetic smart nanopores and nanochannels, Chem. Soc. Rev. 40 (5) (2011) 2385–2401.

[8] C.C. Zhu, Y.F. Teng, G.H. Xie, P. Li, Y.C. Qian, B. Niu, P. Liu, W.P. Chen, X.Y. Kong, L. Jiang, L.P. Wen, Bioinspired hydrogel-based nanofluidic ionic diodes: nano-confined network tuning and ion transport regulation, Chem. Commun. 56 (58) (2020) 8123–8126, https://doi.org/10.1039/D0CC01313G.

[9] P. Ramirez, J. Cervera, V. Gomez, M. Ali, S. Nasir, W. Ensinger, S. Mafe, Optimizing energy transduction of fluctuating signals with nanofluidic diodes and load capacitors, Small 14 (18) (2018) 1702252, https://doi.org/10.1002/smll.201702252.

[10] W.H. Guan, S.X. Li, M.A. Reed, Voltage gated ion and molecule transport in engineered nanochannels: theory, fabrication and applications, Nanotechnol. 25 (12) (2014), 122001, https://doi.org/10.1088/0957-4484/25/12/122001.

[11] W.W. Xin, L. Jiang, L.P. Wen, Two-dimensional nanofluidic membranes toward harvesting salinity gradient power, Acc. Chem. Res. 54 (22) (2021) 4154–4165, https://doi.org/10.1021/acs.accounts.1c00431.

[12] X.D. Huang, X.Y. Kong, L.P. Wen, L. Jiang, Bioinspired ionic diodes: from unipolar to bipolar, Adv. Funct. Mater. 28 (49) (2018) 1801079, https://doi.org/10.1002/adfm.201801079.

[13] G.I. Guerrero-Garcia, F.J. Solis, K. Raidongia, A.R. Koltonow, J.X. Huang, M.O. de la Cruz, Control of selective ion transfer across liquid-liquid interfaces: a rectifying heterojunction based on immiscible electrolytes, ACS Central Sci. 2 (11) (2016) 857–866, https://doi.org/10.1021/acscentsci.6b00266.

[14] K. Mathwig, B.D.B. Aaronson, F. Marken, Ionic transport in microhole fluidic diodes based on asymmetric ionomer film deposits, ChemElectroChem 5 (6) (2018) 897–901, https://doi.org/10.1002/celc.201700464.

[15] B.R. Putra, L. Tshwenya, M.A. Buckingham, J.Y. Chen, K.J. Aoki, K. Mathwig, O. A. Arotiba, A.K. Thompson, Z.K. Li, F. Marken, Microscale ionic diodes: an overview, Electroanalysis 33 (6) (2021) 1398–1418, https://doi.org/10.1002/elan.202060614.

[16] A. Khalil, F.E. Ahmed, N. Hilal, The emerging role of 3D printing in water desalination, Sci. Total Environ. 790 (2021), 148238, https://doi.org/10.1016/j.scitotenv.2021.148238.

[17] H.G. Chun, T.D. Chung, Iontronics, Annu. Rev. Anal. Chem. 8 (2015) 441–462, https://doi.org/10.1146/annurev-anchem-071114-040202.

[18] Y.Q. Hou, X. Hou, Bioinspired nanofluidic iontronics, Science 373 (6555) (2021) 628–629, https://doi.org/10.1126/science.abj0437.

[19] D.P. He, E. Madrid, B.D.B. Aaronson, L. Fan, J. Doughty, K. Mathwig, A.M. Bond, N.B. McKeown, F. Marken, A cationic diode based on asymmetric Nafion film deposits, ACS Appl. Mater. Interfaces 9 (12) (2017) 11272–11278, https://doi.org/10.1021/acsami.7b01774.

[20] B.R. Putra, K. Szot-Karpinska, P. Kudla, H. Yin, J.A. Boswell, A.M. Squires, M.A. Da Silva, K.J. Edler, P.J. Fletcher, S.C. Parker, F. Marken, Bacteriophage M13 aggregation on a microhole poly(ethylene terephthalate) substrate produces an anionic current rectifier: sensitivity toward anionic versus cationic guests, ACS Appl. Bio Mater. 3 (1) (2020) 512–521, https://doi.org/10.1021/acsabm.9b00952.

[21] B.R. Putra, K.J. Aoki, J.Y. Chen, F. Marken, Cationic rectifier based on a graphene oxide-covered microhole: theory and experiment, Langmuir 35 (6) (2019) 2055–2065, https://doi.org/10.1021/acs.langmuir.8b03223.

[22] L. Tshwenya, B.R. Putra, B.O. Orimolade, F. Marken, O.A. Arotiba, Surface modified carbon nanomats provide cationic and anionic rectifier membranes in

aqueous electrolyte media, Electrochim. Acta 354 (2020), 136750, https://doi.org/10.1016/j.electacta.2020.136750.
[23] B.D.B. Aaronson, D. Wigmore, M.A. Johns, J.L. Scott, I. Polikarpov, F. Marken, Cellulose ionics: switching ionic diode responses by surface charge in reconstituted cellulose films, Analyst 142 (19) (2017) 3707–3714, https://doi.org/10.1039/c7an00918f.
[24] Y.Y. Rong, Q.L. Song, F. Marken, pH-induced reversal of ionic diode polarity in 300 nm thin membranes based on a polymer of intrinsic microporosity, Electrochem. Commun. 69 (2016) 41–45, https://doi.org/10.1016/j.elecom.2016.05.019.
[25] B.R. Putra, B.D.B. Aaronson, F. Marken, Ionic diode characteristics at a polymer of intrinsic microporosity (PIM) | nafion "heterojunction" deposit on a microhole poly (ethylene-terephthalate) substrate, Electroanalysis 29 (10) (2017) 2217–2223, https://doi.org/10.1002/elan.201700247.
[26] E. Madrid, P. Cottis, F. Marken, 6-chamber water desalination concept using an ionic rectifier based on a polymer of intrinsic microporosity (PIM), J. Mater. Chem. A 3 (31) (2015) 15849–15853, https://doi.org/10.1039/c5ta04092b.
[27] B.R. Putra, E. Madrid, L. Tshwenya, O.A. Arotiba, F. Marken, An AC-driven desalination/salination system based on a nafion cationic rectifier, Desalination 480 (2020), 114351, https://doi.org/10.1016/j.desal.2020.114351.
[28] K.A. Mauritz, R.B. Moore, State of understanding of nafion, Chem. Rev. 104 (10) (2004) 4535–4585, https://doi.org/10.1021/cr0207123.
[29] D. Henkensmeier, M. Najibah, C. Harms, J. Zitka, J. Hnat, K. Bouzek, Overview: state-of-the art commercial membranes for anion exchange membrane water electrolysis, J. Electrochem. Energy Convers. Stor. 18 (2) (2021), 024001, https://doi.org/10.1115/1.4047963.
[30] H.Z. Yang, J.J. Kaczur, S.D. Sajjad, R.I. Masel, Electrochemical conversion of CO_2 to formic acid utilizing sustainion membranes, J. CO2 Utilizat. 20 (2017) 208–217, https://doi.org/10.1016/j.jcou.2017.04.011.
[31] K.J. Aoki, L. Liu, F. Marken, J.Y. Chen, Rectification effects of nafion-backed micropore-voltammograms by difference in migrational modes, Electrochim. Acta 358 (2020), 136839, https://doi.org/10.1016/j.electacta.2020.136839.
[32] B.D. Coday, T. Luxbacher, A.E. Childress, N. Almaraz, P. Xu, T.Y. Cath, Indirect determination of zeta potential at high ionic strength: specific application to semipermeable polymeric membranes, J. Membr. Sci. 478 (2015) 58–64, https://doi.org/10.1016/j.memsci.2014.12.047.
[33] M.Z. Pan, C.J. Pan, C. Li, J. Zhao, A review of membranes in proton exchange membrane fuel cells: transport phenomena, performance and durability, Renew. Sust. Energ. Rev. 141 (2021), 110771, https://doi.org/10.1016/j.rser.2021.110771.
[34] L. Tshwenya, B.R. Putra, B.O. Orimolade, F. Marken, O.A. Arotiba, Surface modified carbon nanomats provide cationic and anionic rectifier membranes in aqueous electrolyte media, Electrochim. Acta 354 (2020), 136750, https://doi.org/10.1016/j.electacta.2020.136750.
[35] C.G. Zoski, A survey of steady-state microelectrodes and experimental approaches to a voltametric steady-state, J. Electroanal. Chem. 296 (2) (1990) 317–333, https://doi.org/10.1016/0022-0728(90)87256-J.
[36] S.M. Shalaby, S.W. Sharshir, A.E. Kabeel, A.W. Kandeal, H.F. Abosheiasha, M. Abdelgaied, M.H. Hamed, N.U. Yang, Need a reference reverse osmosis desalination systems powered by solar energy: preheating techniques and brine disposal challenges - a detailed review, Energy Conv. Manag. 251 (2022), 114971, https://doi.org/10.1016/j.enconman.2021.114971.